Structural transformation of nascent char during the fast pyrolysis of mallee wood and low-rank coals

Lei Zhang[1], Tingting Li[1], Dimple Quyn[1], Li Dong[1], Penghua Qiu[1,2], Chun-Zhu Li[1,*]

[1]Fuels and Energy Technology Institute, Curtin University of Technology, GPO Box U1987, Perth, WA 6845, Australia

[2]School of Energy Science and Engineering, Harbin Institute of Technology, 92 West Dazhi Street, Harbin, Heilongjiang 150001, People's Republic of China

* Corresponding author:

E-mail address: chun-zhu.li@curtin.edu.au (Chun-Zhu Li)

Phone: +61 8 9266 1131

Fax: +61 8 9266 1138

February 2015

Abstract

The changes in char structure during the fast pyrolysis of three different feedstocks from 600 °C to 1200 °C were investigated. Western Australian Collie sub-bituminous coal, Victorian Loy Yang brown coal and Australian mallee wood were pyrolysed in a wire-mesh reactor at a heating rate of 1000 K s^{-1} with holding time ranging from 0 s to 50 s. FT-Raman/IR spectroscopy was used to characterise the structural features of the chars obtained at different temperatures. The combined use of a wire-mesh reactor and a FT-Raman/IR spectrometer has provided significant insights into the rapid changes in the chemical structure of nascent char during fast pyrolysis. Our results indicate that the three fuels began significant ring condensation at different temperatures. Mallee wood showed significant growth of large rings within 1 s holding at 600 °C; however Loy Yang and Collie coals showed significant ring condensation at 800 °C and 900 °C respectively. With increase in temperature to 1000 °C and higher, most ring condensation occurred at < 1 s holding time. The decrease in the intensity of FT-IR spectrum at ~1600 cm^{-1} confirmed the rapid growth in ring systems at relatively high temperatures.

Keywords: Fast pyrolysis; Char structure; Collie coal;
Loy Yang coal; Mallee wood.

1. Introduction

Gasification is a well-known technology that efficiently converts solid fuels into clean syngas. Biomass and low-rank coals have been considered as suitable feedstocks for gasification due to their high gasification reactivities [1]. Conceptually, fuels undergo two consecutive steps during gasification: the initial fast pyrolysis to produce tar, light gases and nascent char and the subsequent gasification of these products with gasifying agents such as steam, oxygen and carbon dioxide. During the initial gasification, the reactivity of nascent char reduces rapidly when exposed to high temperatures in a gasifier. Further conversion of the char is the rate-controlling step that is relatively slow and determines the overall gasification reactivity [2]. Many factors have been found to correlate with the reduction of char gasification reactivity [2-5].

The structural evolution of char is one of the key factors that results in char deactivation [3-10]. Many techniques have been applied to characterise structural features of char, such as X-ray diffraction (XRD), high-resolution transmission electron microscopy (HRTEM), FT-IR spectroscopy and Raman spectroscopy. FT-Raman spectroscopy is a technique that can detect changes in both crystalline and amorphous carbonaceous structures. In recent studies, it has been used to characterise the chemical structure of chars produced from biomass and low-rank coals during pyrolysis and gasification [6, 9-25].

Previous work showed that there were drastic changes in the structural features of char during the initial stage of gasification when the nascent char only contacted with steam for 20 s (or even possibly shorter) at 700 to 900 °C [10]. For the gasification of Victorian brown coal in steam at 800 °C in a fluidised bed, significant increases in ring condensation occurred during

the initial coal feeding. It was mainly due to thermal annealing and volatile-char interactions [18]. However, little information was obtained about the initial conversion of nascent char structure during pyrolysis or gasification over a wide temperature range.

The transformation of char structure in the early stages of pyrolysis and gasification would also vary with the "rank" of the substrate. Little direct information is currently available in this aspect. For example, it is not clear how differently a nascent char from biomass would behave from a nascent char even from a sub-bituminous coal.

In this study, the changes in the chemical structural features, especially the distribution of aromatic ring systems of nascent chars, were characterised by using FT-Raman/IR spectroscopy. With a wire-mesh reactor, volatile-char interactions were minimised and accurate control of time-temperature history was possible. The aim of this study was to examine (a) the growth of large aromatic rings over a broad range of temperatures (600-1200 °C), (b) the changes in cross-linking structures during fast pyrolysis, and (c) the difference in structural features among three fuels of different rank: biomass, brown coal and sub-bituminous coal.

2. Experimental

2.1 Sample preparation

Three fuels (Western Australian mallee wood, Victorian Loy Yang brown coal and Western Australian Collie sub-bituminous coal) were used in this study. The detailed sample preparation steps can be found elsewhere [9, 26]. The particle size of Loy Yang coal and

Collie coal samples was 106-150 μm, while the particle size of mallee wood sample was 180-400 μm in this study. The properties of these three fuels can be found in Table 1.

2.2 Pyrolysis

A wire-mesh reactor [26-29] was used to carry out the fast pyrolysis experiments. The heating rate was chosen to be 1000 K s^{-1}. Fuel particles were rapidly heated to pre-set temperatures ranging from 600 ° to 1200 °C (accurately measured) followed by a pre-set period of holding up to 50 s. The details of the pyrolysis experiments have been described elsewhere [26, 29]. Briefly, a 325-mesh stainless steel 316 mesh was used as the sample holder. It was preheated to target reaction conditions and proved to have no further weight loss during experiments. Approximately 10 mg of sample was tightly sandwiched between two mesh layers that were then stretched between two electrodes. Two pairs of thermocouple wires were inserted through the meshes at the edge and in the middle of the area where the fuel particles were held. When the sample was heated by an alternating current, the temperature was detected every 0.01 s and provided feedback to the control system. While the sample was being heated, a stream of cool helium (purity > 99.999 vol%) passed through the sample-laden meshes vertically at a flow rate of 0.1 m s^{-1} (measured at 25 °C and 0.1 MPa). This stream of helium would immediately quench the volatiles and take them away from chars, which was responsible for the minimisation of volatile-char interaction. It also allowed the char to be cooled down rapidly to room temperature after experiment, reaching a cooling rate of ~500 K s^{-1} in the range between peak temperature and ~50 °C. After pyrolysis, the weight of char-loaded mesh was weighed and the char was collected.

As the char particles may have fragmented during pyrolysis, especially at high temperatures, some fine particles may have been blown away from the mesh by the high flow rate of helium and thus caused a reduction in the char yield. One test was carried out using each of the three fuels under the extreme experimental conditions (the longest holding time at the highest temperature) used in this study. Prior to heating the sample, the inlet valve of helium was turned off and the experiment was then started immediately. Comparing the char yield with no flow passing through to the char yield with high helium flow rate, the char yields showed only < 1% difference, i.e. within experimental errors. It is implied that the loss of fine particles from mesh during pyrolysis was negligible.

2.3 FT-Raman/IR spectroscopy for char characterisation

A Perkin-Elmer GX FT-Raman/IR spectrometer was used for the characterisation of char structure. The char sample was firstly diluted and ground with spectroscopic grade potassium bromide (KBr). The concentration was chosen so that a plateau value had been reached for the total Raman area, as discussed in [11, 28]. The Raman spectra in the range between 800 and 1800 cm^{-1} were deconvoluted into 10 Gaussian bands by the GRAMS/32 AI software (version 6.0). The assignment of 10 bands has been described in our previous study [11]. The total Raman area, the (G_r+V_l+V_r) band, D band and S band were used to characterise the structural features of nascent char. The strong peak of the FT-IR spectrum at ~1600 cm^{-1} was used in this study to gain some further information about the rapid changes in the aromatic ring systems at high temperatures.

3 Results and discussion

3.1 Char yields of three fuels during fast pyrolysis

Figure 1 shows the char yields of three fuels as a function of holding time at different temperatures. As there were rapid changes in the char yields of three fuels observed during the initial 1 s holding at different temperatures, the x-axis was drawn at a different (expanded) scale, at the holding time between 0 and 1 s, from the rest of the range. All data for the peak temperature of 600 °C in this and all other figures in this paper have been published elsewhere [28] and are only included here for comparison.

In Fig. 1 (a), mallee wood only had a rapid change in char yield during the initial holding at 600 °C within 0.5 s. Further holding at 600 °C or heating to ≥ 800 °C showed negligible changes in the char yield of mallee wood. For the char yields of Loy Yang coal shown in Fig. 1 (b), a significant decrease in the char yield had occurred before the temperature reached 600 °C and 700 °C with 0 s holding time. At 600 °C and 700 °C, the char yield decreased gradually within 50 s holding at 600 °C and 30 s holding at 700 °C. When the Loy Yang coal was heated to 800 °C, a rapid decrease in the char yield was observed during the initial holding at 800 °C at < 0.5 s. However, there is an insignificant change in the weight loss of Loy Yang char after further holding at 800 °C or further heating to higher temperatures. For the char yields from Collie coal in Fig. 1 (c), obvious changes in the char yield happened during the initial holding at the temperatures lower than 800 °C. With the temperature increasing to ≥ 800 °C, lesser changes in char yield were observed than the changes at the temperature < 800 °C.

The data in Fig. 1 show that while the char from the mallee wood reached a plateau char yield at 800 °C, the chars from the brown coal and sub-bituminous coals required much higher temperatures to reach a plateau char yield. These differences are related to the differences in their structure, which will be discussed below. However, it will be noted that the changes in char yield are not always accompanied by the changes in char structure.

3.2 Growth of large ring systems during the fast pyrolysis of three fuels

3.2.1 Changes in the ratio of $I_{(Gr+Vl+Vr)}$ to I_D with char yield

Fig. 2 shows the changes in the ratio of $I_{(Gr+Vl+Vr)}$ to I_D as a function of char yield during the fast pyrolysis of the three fuels at the temperatures from 600 °C to 1200 °C. As the (Gr+Vl+Vr) bands broadly represent "small" aromatics with < 5 fused benzene rings and the D band represents "big" aromatics with ≥6 rings, the ratio between the band areas of (Gr+Vl+Vr) and D bands reflects the ratio between small and large aromatic ring systems in the nascent char [11]. The decrease in the ratio of (Gr+Vl+Vr) to D in Fig. 2 due to: the selective release of small aromatic rings and/or the condensation of small aromatic rings.

In Fig. 2, the changes in $I_{(Gr+Vl+Vr)}/I_D$ had two different stages (slow and rapid) with the changes in char yield. It was manually distinguished by a dotted line and divided into regions A and B in Fig. 2. It is clear that the changes in $I_{(Gr+Vl+Vr)}/I_D$ were much more related to char yield in region A than in region B, reflecting different main reactions taking place in each region.

In region A, the mallee wood and the Loy Yang brown coal showed significant decreases in $I_{(Gr+Vl+Vr)}/I_D$ with the reduction in char yield from ~23% to ~9% and ~55% to ~45%, respectively. These significant changes in ring systems that occurred at 600 °C were discussed in [28], which was more likely attributed to the selective release of small aromatic rings, although the growth of aromatic rings cannot be ruled out. As the changes in ring systems in region A were a strong function of the char yield and the changes in char yield mainly occurred within 1 s of holding at 600 °C (Fig. 1), it indicates that the significant changes in ring systems in region A for the mallee wood and the Loy Yang brown coal mainly occurred during the initial holding at 600 °C. The Collie sub-bituminous coal showed much less changes in ring systems in region A with decreasing char yield from ~75% to ~62% at 600 °C than the other two fuels. It suggests the higher stability of Collie coal char structure compared to the nascent chars from other two feedstocks.

During further weight loss of the Loy Yang coal from ~45% to ~40%, the changes in the ratio of small to large rings became slow. It indicates the char structure became relatively stable at 700-800 °C after the selective decomposition of the active small ring systems in char. For the Collie coal, after the temperature increased to 700 °C and 800 °C, the ratio of small to large rings gradually decreased while the char yield decreased from ~62% to ~58%, which indicates that some small rings might be activated and then released/condensed with the increase in temperature. As shown in Fig. 1 (c), most changes in char yield of Collie coal occurred < 1 s holding at 700 °C and 800 °C. It is inferred that the changes in ring systems of Collie coal due to weight loss mainly happened within < 1 s at 700 °C and 800 °C.

In contrast to the different behaviours for the three fuels in region A, all three fuels showed a rapid decrease in $I_{(Gr+Vl+Vr)}/I_D$ in region B (as is shown in Fig. 2) with insignificant changes in

char yield. In particular, with the decreases in the char yield of mallee wood from ~9% to ~6% in region B, there were very drastic decreases in the ratio of small to large rings from ~3.5 to ~1.5. These significant changes in the ratio were most likely due to ring condensation that might cause massive conversion from small to large rings with the release of very light gases such as H_2. For the Loy Yang brown coal, when the char yield dropped to lower than ~40% in region B, there were also significant decreases in the ratio between small and large rings. With the slight change in char yield from ~40% to ~35%, the ratio of small to large rings decreased significantly from ~2.3 to ~1.3. Similar to the discussion above about mallee wood, the fast reduction in $I_{(Gr+Vl+Vr)}/I_D$ seemed mainly to be due to ring condensation. Similarly, for the Collie sub-bituminous coal, the ratio largely dropped from ~1.8 to ~1.2 while the char yield decreased from 56% to 52% in region B. It should be also mainly due to ring condensation.

As was stated above, the changes in the ring systems of the three fuels in region A were stronger functions of char yield than those in region B. However, with the decrease in $I_{(Gr+Vl+Vr)}/I_D$ in region B, the drastic growth of large aromatic rings due to ring condensation in the three fuels seemed more related to the peak temperature and holding time rather than char yield. The exact reasons will be further discussed in next section. It is important to note here that the temperatures in region B where significant extents of ring condensation began were different among the three fuels. There was drastic ring condensation at 600 °C for mallee wood, 800 °C for Loy Yang brown coal and 900 °C for Collie sub-bituminous coal. In other words, significant ring condensation during fast pyrolysis happened at relatively higher temperature for higher ranked fuels in this study. It may be attributed to the increasing stability of char structure with the increase in fuel rank.

3.2.2 Growth of large aromatic rings by ring condensation

The previous section showed that significant ring condensation occurred during the fast pyrolysis of three fuels at different temperatures. In this section, the changes in $I_{(Gr+Vl+Vr)}/I_D$ ratio as a function of holding time at different temperatures will be discussed, to gain insight into the mechanism of the reaction of ring condensation.

Figure 3 shows the changes in $I_{(Gr+Vl+Vr)}/I_D$ for the three fuels. As discussed in the previous section, the reaction of ring condensation mainly occurred in region B (Fig. 2), which corresponded to the region below the dashed lines in Figs. 3 (a), (b) and (c). For mallee wood shown in Fig. 3 (a), ring condensation gradually took place during holding from 0.5 s to 30 s at 600 °C. With increasing temperature to 800 °C and 1000 °C, a significant decrease of $I_{(Gr+Vl+Vr)}/I_D$ was observed with 0 s holding at 800 °C and < 0.5 s holding at 1000 °C. Although there were gradual increases in ring condensation during further holding at 800 °C and 1000 °C, the differences in $I_{(Gr+Vl+Vr)}/I_D$ at different temperatures were firstly observed during the initial holding (< 0.5 s) at peak temperatures.

The change in $I_{(Gr+Vl+Vr)}/I_D$ for the two coals were similar. The ring condensation rate was slow at relatively low temperatures (Loy Yang coal at 800 °C and Collie coal at 900 °C). However, with the rise of temperature, the reaction rates of ring condensation seemed to become increasingly fast. At high temperatures such as 1000 °C, most changes in the conversion of small to large rings in three fuels are completed within < 0.5 s holding time. Furthermore, although the distribution of the ring systems in the three fuels was very different during the initial pyrolysis at 600 °C, $I_{(Gr+Vl+Vr)}/I_D$ of three fuels approached to each other at the temperature ≥ 1000 °C.

3.3 Changes in the total Raman area during fast pyrolysis

Figure 4 shows the changes in the total Raman area as a function of holding time at the temperature from 600 °C to 1200 °C. There may be two key factors causing the total Raman area to decrease during the pyrolysis [11]. The loss of O-containing functional groups would largely decrease the resonance effects to reduce the observed Raman intensity. Further, the condensation of aromatic ring systems would greatly increase the light absorptivity, which in turn would decrease the total Raman intensity.

In Fig. 4 (a), the total Raman area of the mallee wood char gradually decreased during holding at 600 °C and rapidly reduced during the initial holding at 800 °C and 1000 °C; this shows some correlation with the increase in ring condensation shown in Fig. 3 (a). It also indicates that the loss of O-containing functional groups occurred simultaneously with ring condensation for mallee wood. As for the Loy Yang coal shown in Fig. 4 (b), when the temperature increased to ≥ 700 °C, similar to the mallee wood, the decrease in total Raman area was largely related to ring condensation shown in Fig. 3 (b). For the Collie coal shown in Fig. 4 (c), the total Raman area changed rapidly at temperatures < 900 °C, while there were insignificant changes in ring systems during holding at this temperature range. Therefore, the rapid change in the total Raman area of Collie coal char was mainly due to the loss of O-containing functional groups and it happened before the significant growth of large aromatic rings. Comparing the three fuels, it can be inferred that deoxygenation proceeded together with ring condensation for the lower-ranked fuels (e.g. mallee wood and Loy Yang coal) and occurred before ring condensation for the relatively higher-ranked fuel (e.g. Collie coal).

3.4 Confirmation of fast growth of large aromatic rings

The IR spectrum near 1600 cm^{-1} is usually the strongest band in coal char. It is assigned mainly as aromatic C=C stretching [30, 31]. Our previous study on the gasification of Loy Yang coal in CO_2 and O_2 also indicated that this band was mainly attributed to the aromatic C=C stretching [14]. As discussed above, a fast growth in large aromatic rings in the three fuels was observed during the initial holding at high temperatures. With the aromatisation of nascent char, the size of ring systems increases and the aromatic C=C stretching can be restricted. Due to this, the IR band near 1600 cm^{-1} may have a significant drop during rapid ring condensation.

Fig. 5 shows the changes in IR spectra of the nascent char of the two coals between 1800 and 1500 cm^{-1} during holding at high temperatures. The IR band of Loy Yang coal char at 1600 cm^{-1} showed a significant decrease at 800 ℃ within 1 s holding. With the temperature increase to 1000 ℃ in Fig. 5 (b), a significant decrease of this band occurred within 0.5 s， which was in accordance with the fast ring condensation at high temperature shown in Fig. 3 (b). Collie coal char exhibited a similar phenomenon to that of Loy Yang coal char. With the rapid changes in the ring systems at 900 ℃ and 1000 ℃ shown in Figs. 5 (c) and (d), Collie coal char showed a significant decrease in the intensity of IR spectrum at ~1600 cm^{-1} within 1 s at 900 ℃ and within even 0.1 s at 1000 ℃. Therefore, the fast changes at ~1600 cm^{-1} in the IR spectrum of nascent chars confirmed the rapid and significant growth in large aromatic ring systems during fast pyrolysis, as discussed in the previous sections.

Mallee wood nascent char had strong bands at ~1400 cm^{-1} (shown in Fig. 6) that may be attributed to the very high concentration of oxygen or potassium in mallee wood [9, 32]. The

band at ~1400 cm^{-1} largely overlaps the band at ~1600 cm^{-1} for mallee wood chars. Nevertheless, the changes in IR spectra of mallee wood char at ~1600 cm^{-1} are in broad agreement with those of coals.

320

3.5 Changes in cross-linking structure during fast pyrolysis

Fig. 7 shows the change in the ratio between the intensity of the S band (I_S) and the overall intensity ($I_{\text{total Raman area}}$) in the region of 800 cm^{-1}-1800 cm^{-1} as a function of holding time at
325 different temperatures. The ratio of I_S to $I_{\text{total Raman area}}$ gives an indication of cross-linking structures in the char matrix [11]. It is clear that all three fuels show a significant increase in $I_S/I_{\text{total Raman area}}$ during holding at the temperature < 800 °C when there is significant thermal decomposition as shown in Fig. 1. It indicates that the thermal breakdown of some active groups (e.g. carboxyl and alkyl groups) created more free sites on char matrix that reconnect
330 and form stable cross-linking structures. However, with the temperature increasing to $\geqslant$ 800 °C, all three fuels showed insignificant changes in the ratio of I_S to $I_{\text{total Raman area}}$. It suggests that many cross-linking structures that are formed at relatively low temperature are very stable even at 1200 °C during holding up to 5 s. Although some cross-linking structures might be broken at high temperature with reactions such as ring condensation, new cross-
335 linking structures would form to preserve a stable carbon skeleton.

4. Conclusions

The changes in nascent char structure during the fast pyrolysis at temperatures from 600 °C
340 to 1200 °C have been studied by combined features of a wire-mesh reactor with FT-Raman/IR spectroscopy.

1. There were insignificant changes in char yield at the temperatures > 600 ℃ for the mallee wood, > 800 ℃ for the Loy Yang brown coal and > 900 ℃ for the Collie sub-bituminous coal. However, significant decreases in the ratio of small to large rings occurred at these temperature ranges for the three fuels. The negligible change in char yield with a corresponding large decrease in the ratio of small to large rings is most likely attributed to ring condensation.

2. With increasing temperature, ring condensation would largely occur within very short holding times. For all three fuels, most of the ring condensation was observed within 0.1s holding at temperatures ≥ 1000 ℃.

3. Although the distribution of the ring systems in the chars from these three fuels was largely different during the initial pyrolysis at 600 ℃, their $I_{(Gr+Vl+Vr)}/I_D$ values were very close at temperatures ≥ 1000 ℃.

4. The fast decrease in the FT-IR intensity of nascent char at ~1600 cm^{-1} corresponded to the rapid growth of large aromatic ring systems at the temperature ≥ 800 ℃ for Loy Yang coal and ≥ 900 ℃ for Collie coal. It supported the rapid enhancement of ring condensation at relatively high temperatures for two coals.

5. The formation of cross-linking structure was significant during holding at temperatures from 600 ℃ to 800 ℃ for all three fuels. The relative small changes in the cross-linking structure at high temperatures suggest that there may have some cross-linking structures broken at high temperatures with new cross-linking formed afterwards.

Acknowledgements

The authors gratefully acknowledge the financial support of this study from the Australian Research Council (DP110105514), the Commonwealth of Australia under the Australia-China Science and Research Fund and WA Department of Mines and Petroleum. The authors also gratefully thank Muja power plant for providing Collie raw coal. This research used samples of mallee biomass supplied without cost by David Pass and Wendy Hobley, from their property in the West Brookton district.

References

[1] C.-Z. Li, Special issue-gasification: a route to clean energy, Process Safety and Environmental Protection 84 (2006) 407-408.

[2] K. Miura, K. Hashimoto, P.L. Silveston, Factors affecting the reactivity of coal char during gasification, and indices representing reactivity, Fuel 68 (1989) 1461-1475.

[3] C.-Z. Li, Some recent advances in the understanding of pyrolysis and gasification behaviour of Victorian brown coal, Fuel 86 (2007) 1664-1683.

[4] O. Senneca, P. Salatino, S. Masi, Microstructural changes and loss of gasification reactivity of chars upon heat treatment, Fuel 77 (1998) 1483-1493.

[5] H. Wu, J.-I. Hayashi, T. Chiba, T. Takarada, C.-Z. Li, Volatilisation and catalytic effects of alkali and alkaline earth metallic species during the pyrolysis and gasification of Victorian brown coal. Part V. Combined effects of Na concentration and char structure on char reactivity, Fuel 83 (2004) 23-30.

[6] C. Sheng, Char structure characterised by Raman spectroscopy and its correlations with combustion reactivity, Fuel 86 (2007) 2316-2324.

[7] B. Feng, S.K. Bhatia, J.C. Barry, Structural ordering of coal char during heat treatment and its impact on reactivity, Carbon 40 (2002) 481-496.

[8] A. Sharma, H. Kadooka, T. Kyotani, A. Tomita, Effect of microstructural changes on gasification reactivity of coal chars during low temperature gasification, Energy & Fuels 16 (2002) 54-61.

[9] M. Asadullah, S. Zhang, Z. Min, P. Yimsiri, C.-Z. Li, Effects of biomass char structure on its gasification reactivity, Bioresource Technology 101 (2010) 7935-7943.

[10] D.M. Keown, J.-I. Hayashi, C.-Z. Li, Drastic changes in biomass char structure and reactivity upon contact with steam, Fuel 87 (2008) 1127-1132.

[11] X. Li, J.-I. Hayashi, C.-Z. Li, FT-Raman spectroscopic study of the evolution of char structure during the pyrolysis of a Victorian brown coal, Fuel 85 (2006) 1700-1707.

[12] X. Li, C.-Z. Li, Volatilisation and catalytic effects of alkali and alkaline earth metallic species during the pyrolysis and gasification of Victorian brown coal. Part VIII. Catalysis and changes in char structure during gasification in steam, Fuel 85 (2006) 1518-1525.

[13] X. Li, J.-I. Hayashi, C.-Z. Li, Volatilisation and catalytic effects of alkali and alkaline earth metallic species during the pyrolysis and gasification of Victorian brown coal. Part VII. Raman spectroscopic study on the changes in char structure during the catalytic gasification in air, Fuel 85 (2006) 1509-1517.

[14] H.-L. Tay, C.-Z. Li, Changes in char reactivity and structure during the gasification of a Victorian brown coal: Comparison between gasification in O_2 and CO_2, Fuel Processing Technology 91 (2010) 800-804.

[15] X. Guo, H.-L. Tay, S. Zhang, C.-Z. Li, Changes in char structure during the gasification of a Victorian brown coal in steam and Oxygen at 800 °C, Energy & Fuels 22 (2008) 4034-4038.

[16] H.-L. Tay, S. Kajitani, S. Zhang, C.-Z. Li, Effects of gasifying agent on the evolution of char structure during the gasification of Victorian brown coal, Fuel 103 (2013) 22-28.

[17] S. Zhang, Z. Min, H.-L. Tay, Y. Wang, L. Dong, C.-Z. Li, Changes in char structure during the gasification of mallee wood: effects of particle size and steam supply, Energy & Fuels 26 (2012) 193-198.

[18] S. Zhang, Z. Min, H.-L. Tay, M. Asadullah, C.-Z. Li, Effects of volatile-char interactions on the evolution of char structure during the gasification of Victorian brown coal in steam, Fuel 90 (2011) 1529-1535.

[19] T. Li, L. Zhang, L. Dong, C.-Z. Li, Effects of gasification atmosphere and temperature on char structural evolution during the gasification of Collie sub-bituminous coal, Fuel 117 (2014) 1190-1195.

[20] S. Dong, P. Alvarez, N. Paterson, D.R. Dugwell, R. kandiyoti, Study on the effect of heat treatment and gasification on the carbon structure of coal chars and metallurgical cokes using Fourier Transform Raman spectroscopy, Energy and Fuels 23 (2009) 1651-1661.

[21] X. Gong, Z. Guo, Z. Wang, Variation of char structure during anthracite pyrolysis catalyzed by F_2O_3 and its influence on char combustion reactivity, Energy and Fuels 23 (2009) 4547-4552.

[22] X. Zhu, C. Sheng, Influences of carbon structure on the reactivities of lignite char reacting with CO_2 and NO, Fuel Processing Technology 91 (2010) 837-842.

[23] X. Liu, M. Xu, J. Si, Y. Gu, C. Xiong, H. Yao, Effect of sodium on the structure and reactivity of the chars formed under N_2 and CO_2 atmospheres, Energy and Fuels 26 (2012) 185-192.

[24] Z. Wu, S. Wang, J. Zhang, L. Chen, H. Meng, Thermal behaviour and char structure evolution of bituminous coal blends with edible fungi residue during co-pyrolysis, Energy and Fuels 28 (2014) 1792-1801.

[25] X. Qi, X. Guo, L. Xue, C. Zheng, Effect of iron on Shenfu coal char structure and its influence on gasification reactivity, Journal of Analytical and Applied Pyrolysis 110 (2014) 401-407.

[26] C. Sathe, Y. Pang, C.-Z. Li, Effect of heating rate and ion-exchangeable cations on the pyrolysis yields from a Victorian brown coal, Energy & Fuels 13 (1999) 748-755.

[27] K. Jamil, J.-I. Hayashi, C.-Z. Li, Pyrolysis of a Victorian brown coal and gasification of nascent char in CO_2 atmosphere in a wire-mesh reactor, Fuel 83 (2004) 833-843.

[28] L. Zhang, T. Li, D. Quyn, L. Dong, P. Qiu, C.-Z. Li, Formation of nascent char structure during the fast pyrolysis of mallee wood and low-rank coals, Fuel 150 (2015) 486-492.

[29] J.R. Gibbins, R.A.V. King, R.J. Wood, R. Kandiyoti, Variable-heating-rate wire-mesh pyrolysis apparatus, Review of Scientific Instruments 60 (1989) 1129-1139.

[30] A. Koch, A. Krzton, G. Finqueneisel, O. Heintz, J.-V. Weber and T. Zimny, A study of carbonaceous char oxidation in air by semi-quantitative FTIR spectroscopy, Fuel 77 (1998) 563-569.

[31] P.C. Painter, M. Starsinic, E. Squires, A.A Davis, Concerning the 1600 cm^{-1} region in the i.r. spectrum of coal, Fuel 62 (1983) 742-744.

[32] S.J. Yuh, E.E. Wolf, FTIR studies of potassium catalyst-treated gasified coal chars and carbons, Fuel 62 (1983) 252-255.

Table 1 Properties of three fuels [9,14,19]

	Proximate analysis (wt%)		Ultimate analysis (wt%)				
	Ash[a]	Volatile matter[b]	C[b]	H[b]	N[b]	S[b]	O[b.c]
Mallee wood	0.9	81.6	48.2	6.1	0.2	0.0	45.5
Loy Yang coal	1.1	52.2	70.4	5.4	0.62	0.28	23.2
Collie coal	5.7	38.8	75.7	4.5	1.4	0.5	17.9

(a, dry basis; b, dry and ash-free basis; c, by difference)

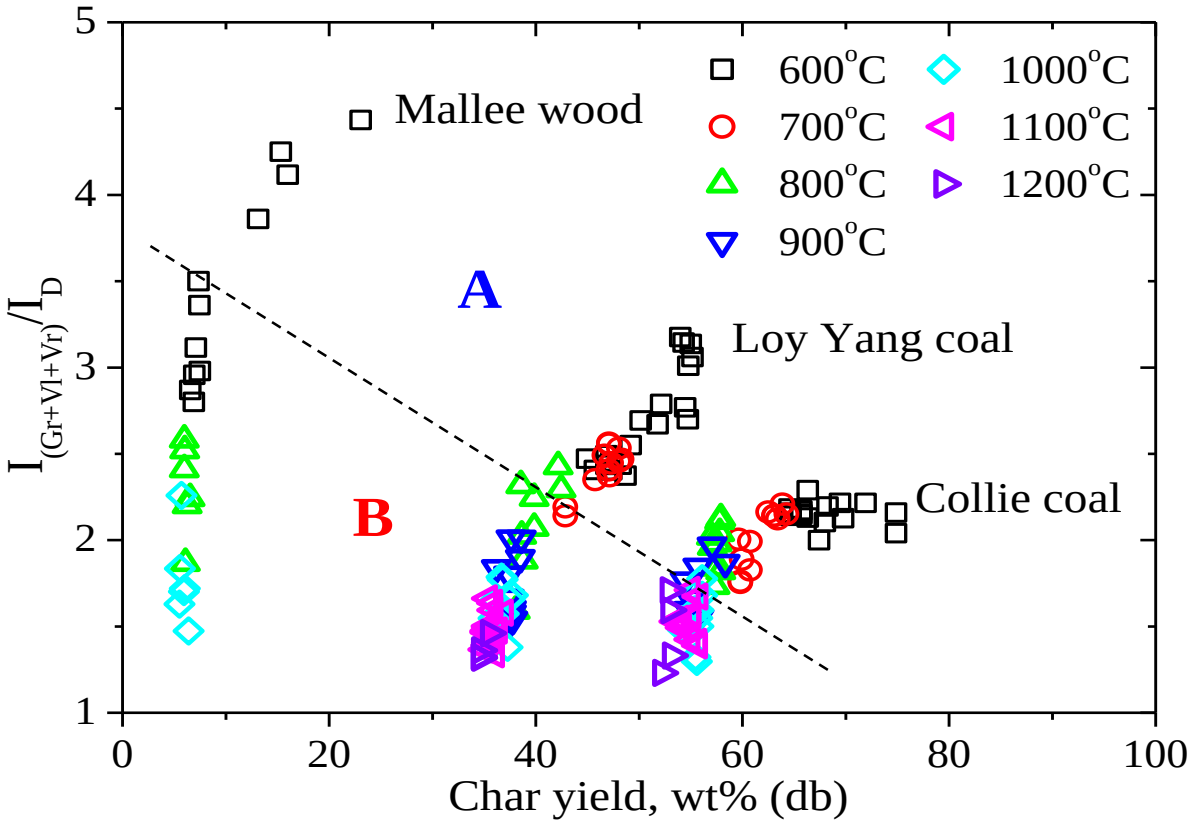
600°C
700°C
800°C
900°C
1000°C
1100°C
1200°C
Mallee wood
Loy Yang coal
Collie coal
A
B
I(Gr+Vl+Vr)/ID
Char yield, wt% (db)
0
20
40
60
80
100
1
2
3
4
5

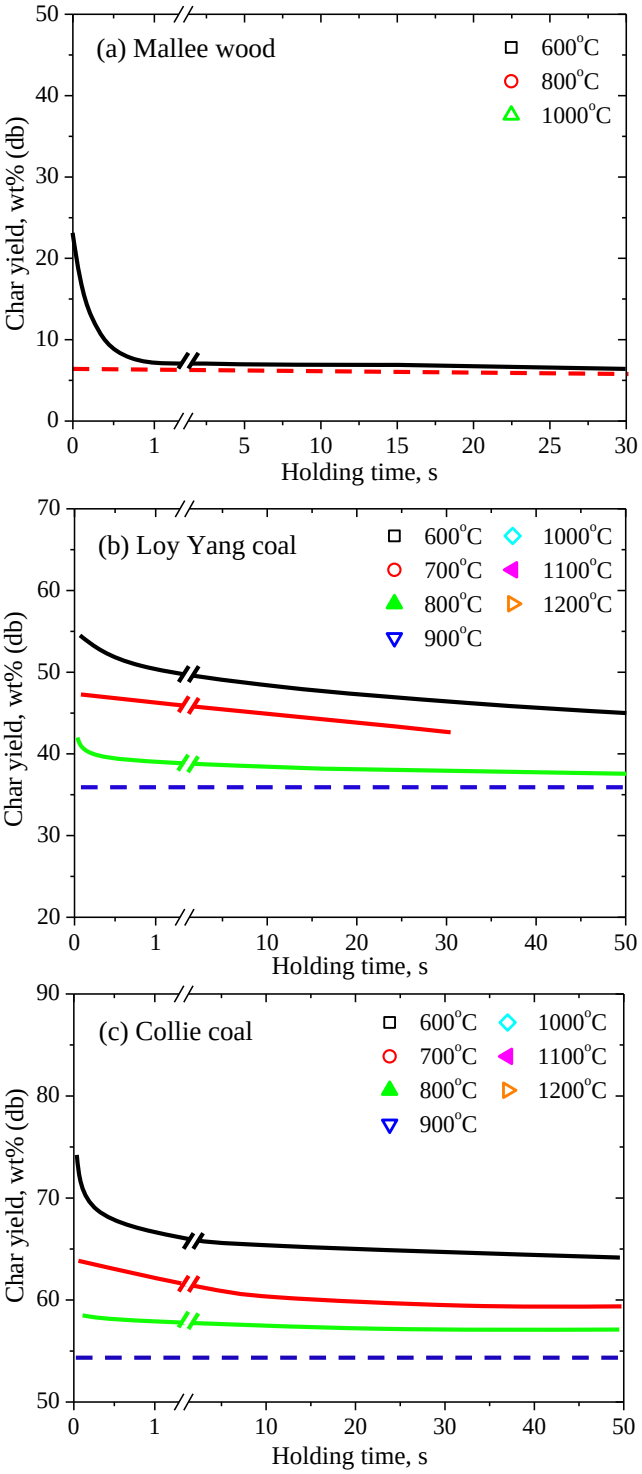

Fig. 1. Char yields of three fuels as a function of holding time and temperature. The data for 600 °C were published before [28] and are shown here for comparison.

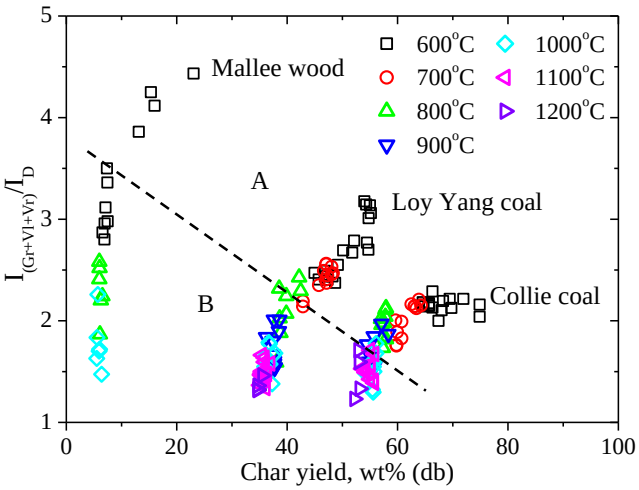

Fig. 2. Changes in the ratio of $I_{(Gr+Vl+Vr)}$ to I_D as a function of char yield. The data for 600 °C were published before [28] and are shown here for comparison.

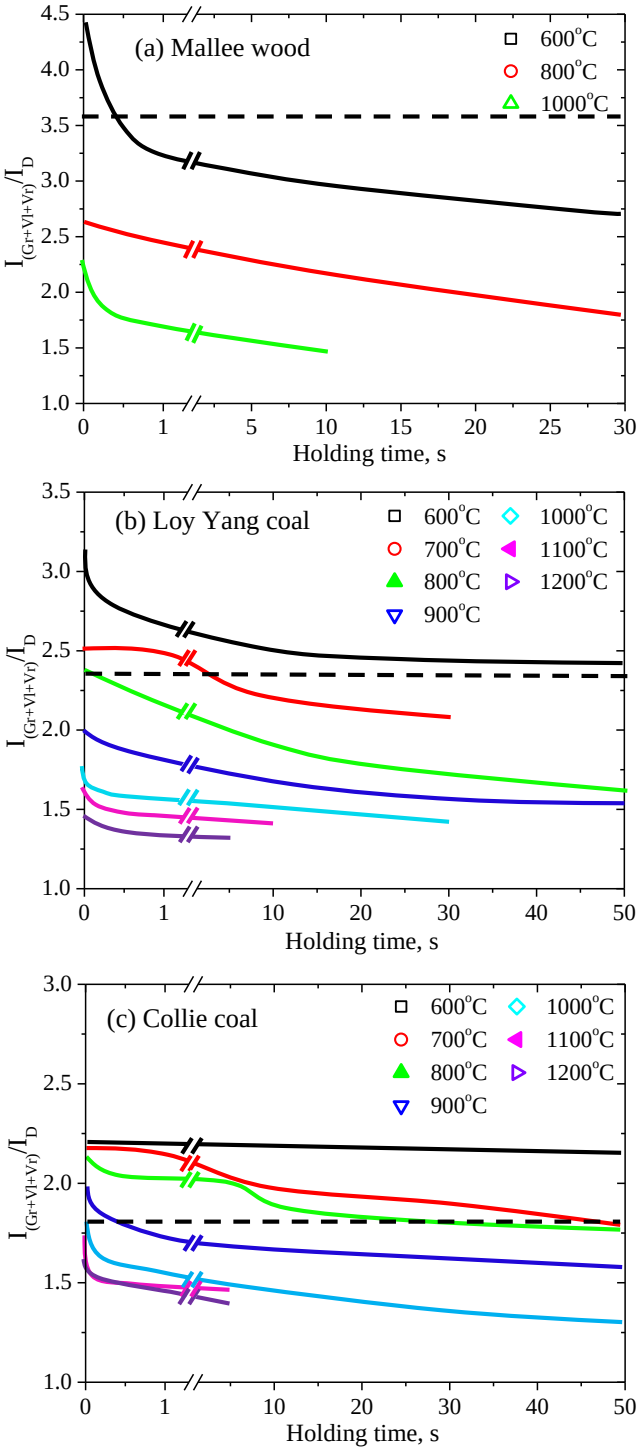

Fig. 3. Ratios between small and large rings of three fuels as a function of holding time and temperature. The data for 600 °C were published before [28] and are shown here for comparison.

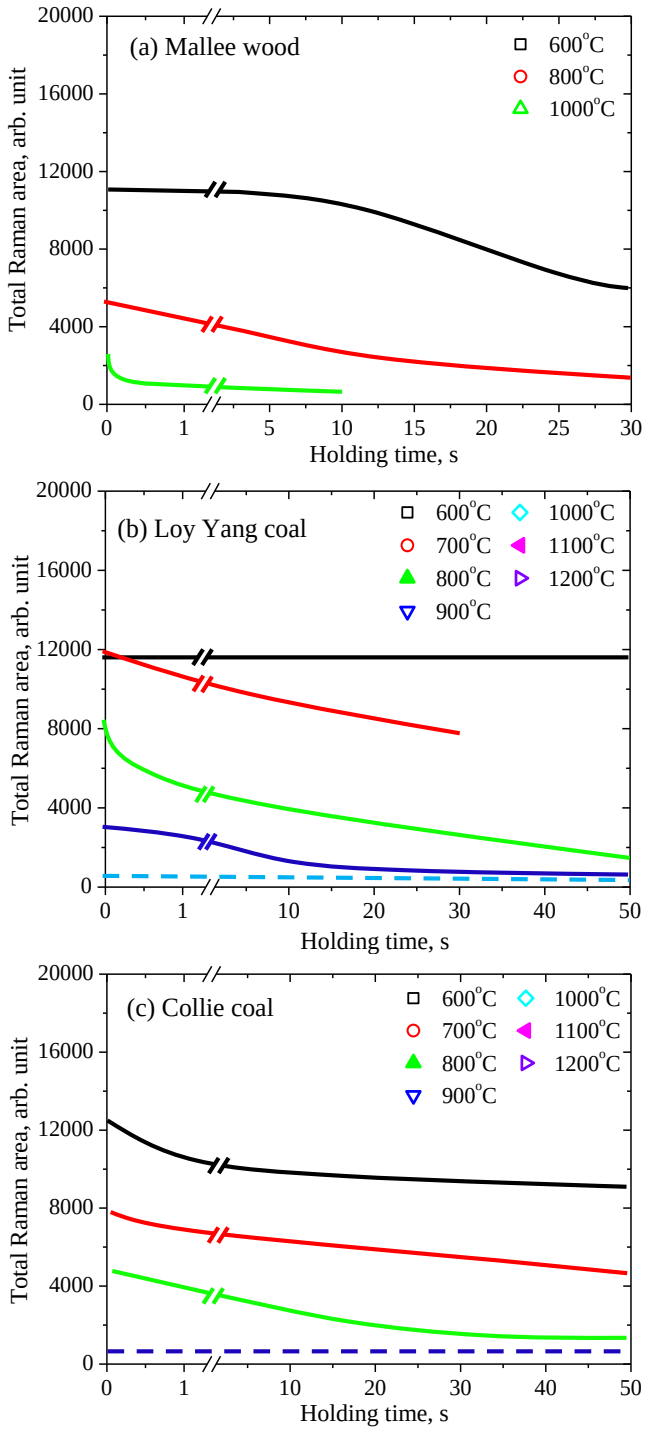

Fig. 4. Total Raman areas between 800 and 1800 cm^{-1} as a function of holding time and temperatures. The data for 600 °C were published before [28] and are shown here for comparison.

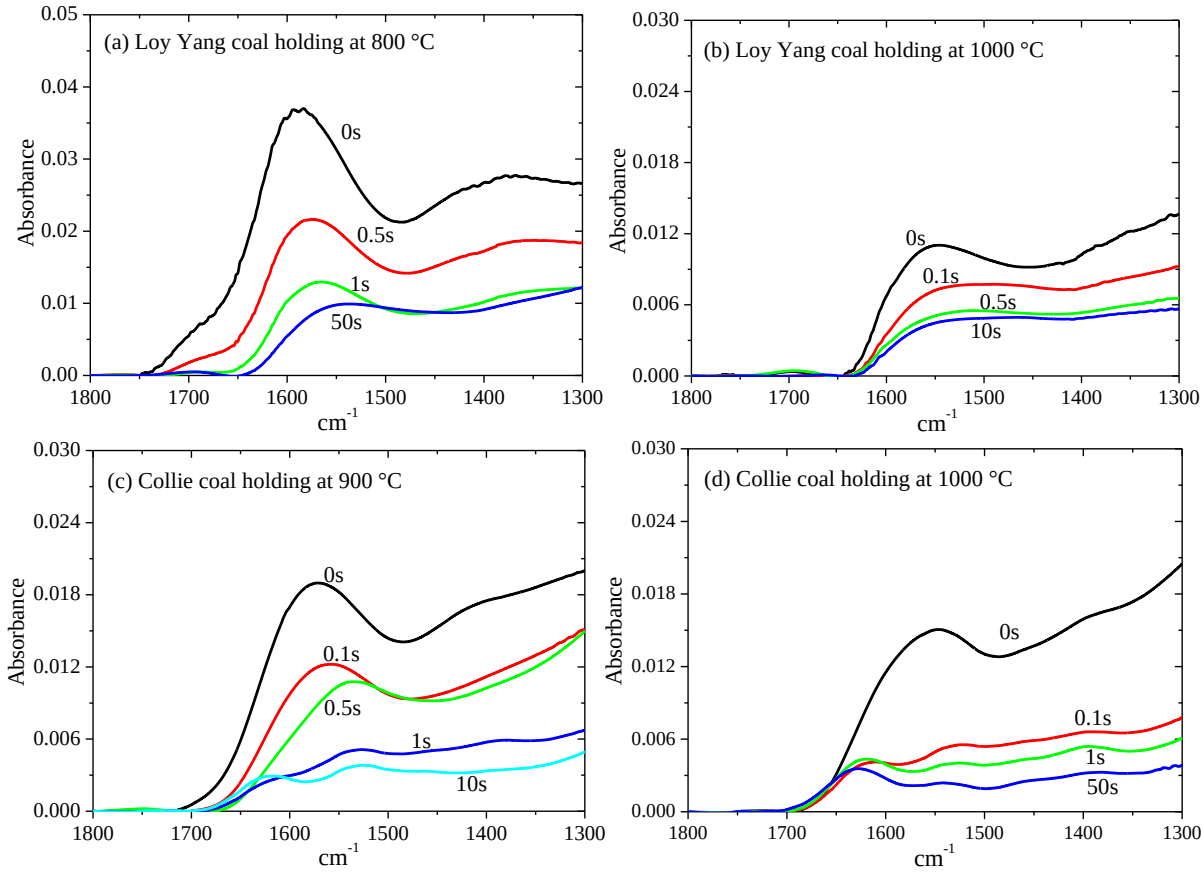

Fig. 5. FT-IR spectra between 1800 and 1300 cm^{-1} of the coal chars.

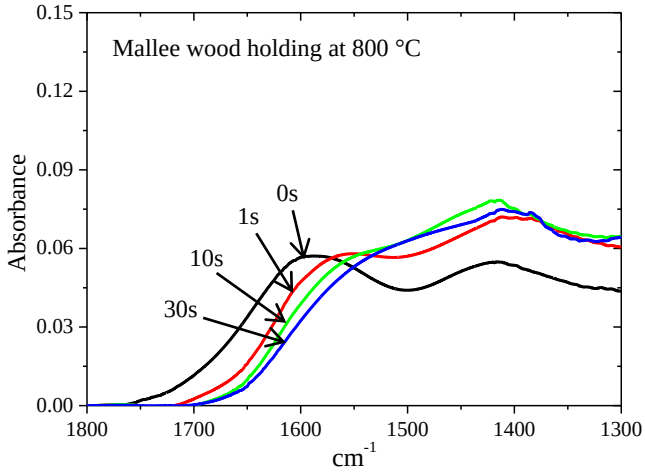

Fig. 6. FT-IR spectra between 1800 and 1300 cm^{-1} of the mallee wood chars.

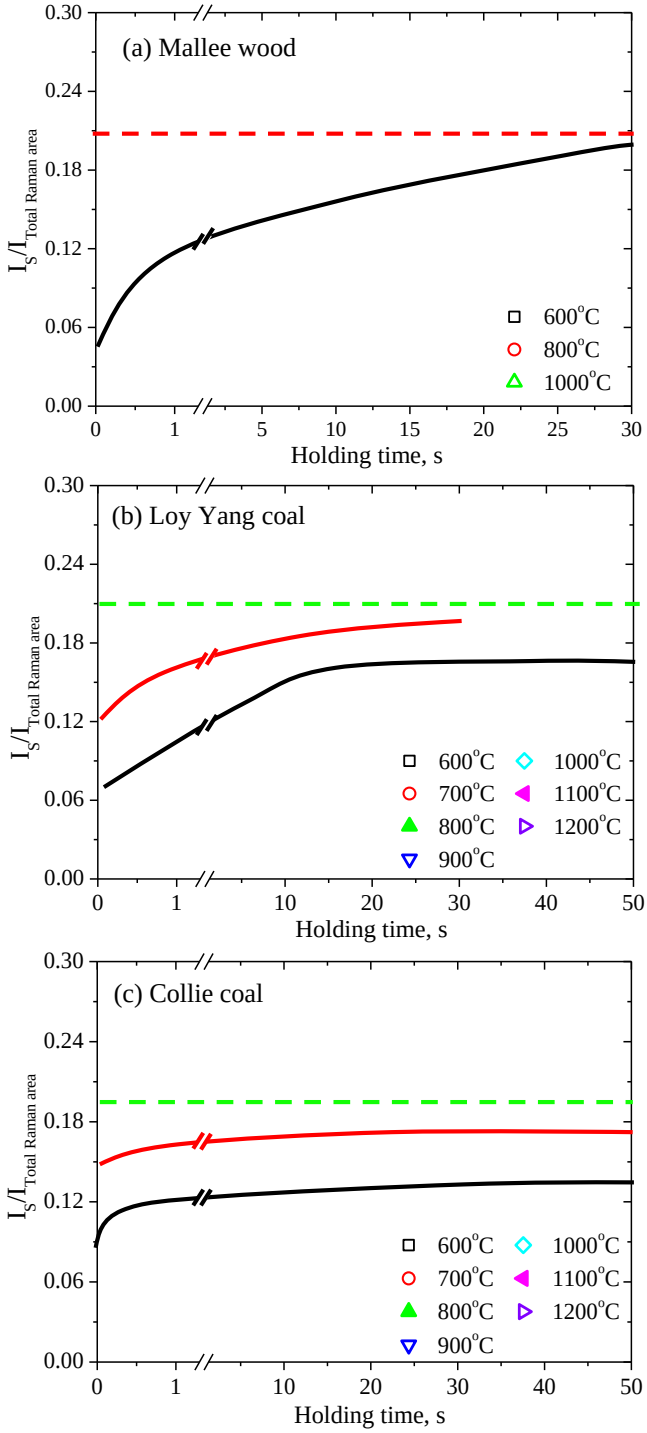

Fig. 7. The relative S band intensities of three fuels as a function of holding time and temperature. The data for 600 °C were published before [28] and are shown here for comparison.

- This study aims to investigate the structural changes in three fuels during fast pyrolysis at temperature from 600 °C to 1200 °C.
- Three fuels start significant condensation of aromatic rings at different temperatures (mallee wood < Loy Yang coal < Collie coal).
- With increasing temperature, ring condensation would largely occur within very short holding time.